

Investigation of cutting tool diameter influencing wire cutting operation accuracy using several matrix configurations

R. Dundulis*, R. Bortkevičius**

*Kaunas University of Technology, Studentų 56, 51424 Kaunas, Lithuania, E-mail: romualdas.dundulis@ktu.lt

**Kaunas University of Applied Engineering Sciences, Tvirtovės al. 35, LT-50155 Kaunas, Lithuania, E-mail: rytis.bortkevicius@edu.ktk.lt

crossref <http://dx.doi.org/10.5755/j01.mech.21.6.13477>

1. Introduction

Process description and actuality of the work. In the paper there is presented an investigation from JSC ITAB NOVENA manufactured products, containing shape disalignments, i.e. cutting wire strip with oval matrix and the punch cannot ensure needed geometric form, therefore it is in need to propose the other geometric shape tools: bigger form of cutting tools. In the paper it is discussed various punch/matrix ratio influence to the wire strip endings area and it's precision. The researches have been conducted using several matrix diametric configuration. Here in presented deformational characteristically curves using various diameters ovalic cutting tools. There were used various diameters wire strip diameters specimens.

The objective of the investigation is to determine the most effective methods to turn strip endings to ovals since at the present time it is getting into sort of shape of triangular. Three main problems were investigated: 1 - the change of cross-sectional area in the cutting place, 2 - bending angle, 3 - monotonous strain distribution in the axial direction of wire strip. Cutting operation were investigated by scientists [1], where is described full formation of the chip in the cutting operation, described material models used in the modelling orthogonal cut [2], elements for modelling cutting operation is fully presented by scientists [3, 4] which models are for used for cutting and also include high strain rates and plastic deformation therefore are replicated with our investigation. One parameter is missing in the works of scientists - material changes in its initial geometry when harder tool initiates a cut [5]. Orthogonal cut is investigated in the scientific works [6, 7, 8]. Here in cutting operation presented when the sharp tool cuts softer material. Major problem of investigation must be considering how rank angle influence the penetration depth [7, 8]. And later on forms a chip. No change in initial geometry are observed. Major object of orthogonal cut is to determine right tool geometry to cut materials with minimized cutting force, and to reduce friction to the lowest possible values [1, 2, 9]. There is a lack of investigation when material is cut with a tool which rank angle is at 90°.

Problem. During normal workday, factory worker cuts several thousand wires strips, which later on goes to the end-customer. The end customer wants to buy thousand wire-strips of different diameter. In order to cut wanted diameter it needed to over-change the punch and the matrix, which is suited for the only particular wire diameter. The end customer started to comply about the quality of the wire strip ends. So the major problem of the investigation is the changed geometry of wire strip endings after the

cutting operation. Therefore, the object of the investigation is wire strip endings and the determination of the right cutting tool.

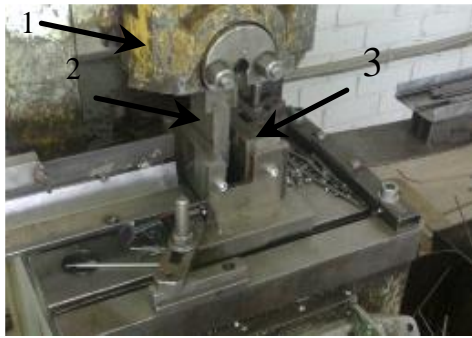
Novelty. The rank angle is considered as obtuse angle [4, 9]. In the present investigation material is cut with mentioned rake angle, so actual cutting operation it is hard to describe. Three phases of cutting operation where there founded and investigated. Some of the problems are related with a modelling in itself. In the past years cutting operation where were modelling with solid elements in three dimensions [4, 8]. Recent years scientists [10, 11, 12, 13, 14] tries to use SPH modelling of cutting operation.

Paper ends up with determined mechanical characteristics of specimens. Identified 3 critical zones where most likely the fracture will occur and begins. In these 3 zones plastic deformation distributed not evenly. In those zones there were measured specimens area reduction and compared with plastic deformation distribution and variation. Accordingly, the most important set of plastic strain ratio were determined.

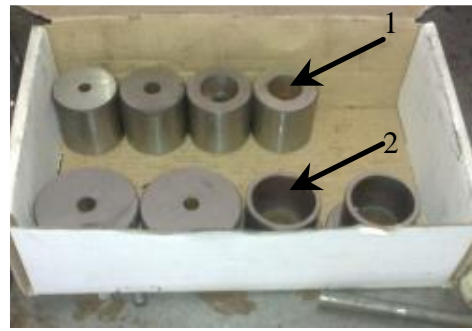
2. Testing procedures

In order to determine the best available quality for wire cutting operation there was constructed wire cutting tool, where major components consisted of classical cutting equipment: the tool holder 1 (it is a main equipment for force supplying), the punch 2 and the matrix 3. It can be seen in the Fig. 1, a.

The punch and the matrix configuration suited only for specific wire diameter and it can be seen in the Fig. 1, b. Here in number 1 designated exchangeable matrix tools and 2 designated exchangeable punch tools. In order to make an investigation there were choosing several simple wire components raging in diameter from Ø2 to Ø6 mm. Several different types of cutting equipment there were tested in order to find the best economically based and quality based solution. To make research in to more deep there was conducted an experiment with equipment stored in the company JSC "ITAB NOVENA" and all copyrights of used equipment solely be-long to the mentioned company. Cut cross section view of the wire strip with a tool (Fig. 1) are given in the Fig. 2. Here in are indicated 3 crucial zones after cutting operation. Experimental measuring of cross section was made using 3D scanner with scanning processing precision of 0.2 µm. 3D scanned view of the wire strip with 3 significant areas can be seen in the Fig. 3, a. The same wire strip has been photographed with ordinary camera. Photo can be seen in the Fig. 3, b. The results of measuring fully matches between scanned object

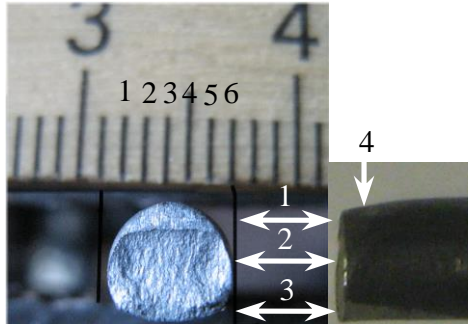


a



b

Fig. 1 Wire cutting tool: a - assembly apparatus; b - exchangeable part for various wire diameters



a

b

Fig. 2 Wire strip cut with oval shape tools excludes four zones of deformation: a - cut zone cross-section view; b - cut zone side view (here can be seen the 4th zone of deformation)

and measured with properties though specimens were taken from one Kaunas Mechel factory. Material to produce wires are delivered from single supplier in the Russian federation. Withdrawn in Kaunas Mechel factory as well as made final heat treatment. Material grade to make a wire identified in the Table 1.

Table 1

Technical specification

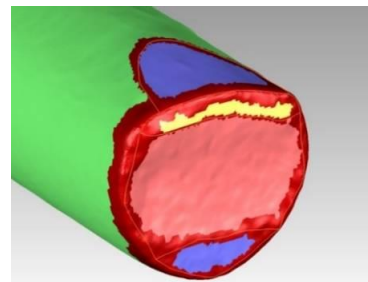
Ø, mm	Tensile strength, MPa	Standard for steel product	Steel grade	Standard for chemical composition
1.0-1.8	1000-1200	EN 10218-2 (DIN 177)	SAE 1006;	ASTM A 510M
2.0-6.0	590-830		SAE 1008	

Therefore, mechanical properties between wire should be identical but it is not so. In order to complete investigation of chosen materials there was in need to complete an investigation of tension test. Investigation were accomplished in the Kaunas University of Technology. Tension test machine grippers were specially constructed for given wire strips. Special form of grippers was designed in order to clamp wire strips between clutches in order to create no movement there in. Several designs of clutches were introduced to make an experiment, but only one was suited for particular experimental studies. Tested material mechanical properties are given in the Table 1. In the both Figs. 2 and 3 there is and the 4th zone, which must be treated as non-perfect and so has to be treated as defect.

Though this 4th zone is not included in cross-sectional measurements but it is very important. As a matter of fact, all deformed specimens have had similar shape of deformed 4th zone. The shape replicates the shape of parabola.

Zones in the cut area do not replicated any known shape describable by any canonical equation. It need to mention, that the 4th zone has identical deformation no matter of cutting tool diameter and wire strip diameter itself. The material properties in the investigation of various specimens there were gained not identical mechanical properties though specimens were taken from one Kaunas Mechel factory.

In the Table 2 indexes denote: σ_p is limit of proportionality, MPa; e_y is yield strain component of the tested material; σ_y is yield stress component of the tested material, MPa; σ_u is ultimate stress state, MPa; e_u is ultimate strain state; σ_f is stress at fracture, MPa; E is Young modulus, MPa Wire specimen no indicate the tested material rank number and figures beside rank number indicate tested material diameter.



a



b

Fig. 3 Cross-section of the Ø5 wire strip with significant areas after cutting operation: a - 3D scan, b - ordinary photograph view

Mechanical characteristics of tested specimens

Wire specimen number	Diameter of wire, mm	σ_p , MPa	e_y	σ_Y , MPa	σ_{it} , MPa	e_u	σ_f , MPa	E , MPa
No.1	2.2	580	0.0029	915	936	0.00482	1190	196756
No.2	2.5	500	0.0028	784	802	0.0049	1160	177368
No.3	3.06	530	0.00313	750	789	0.00828	1119	169276
No.4	3.4	560	0.0033	838	862	0.00843	1169	169910
No.5	4	440	0.002	705	727	0.0071	1004	215651
No.6	5	440	0.0022	710	741	0.0063	1081	196612
No.7	6	360	0.0021	590	623	0.0088	1070	171626

3. Investigation of cutting operation by FEM

Finite element model was created using FEM software LS-Dyna [4, 6]. This model can be analysed in the Fig. 4. FEM model consist of the following equipment: 1 - exchangeable punch, 2 - ex-changeable matrix, and 3 is wire strip. In order to check whether the oval shape is the best available shape for cutting operation there were proposed other cutting shapes: hybrid 1 (consisting from oval punch, which diameter equal to the cutting material diameter and the matrix which diameter is bigger than cutting material diameter).

These shapes are presented in the Fig. 5. The investigation was carried out using several (in this experimental studies we were using 5 different matrix diameters)

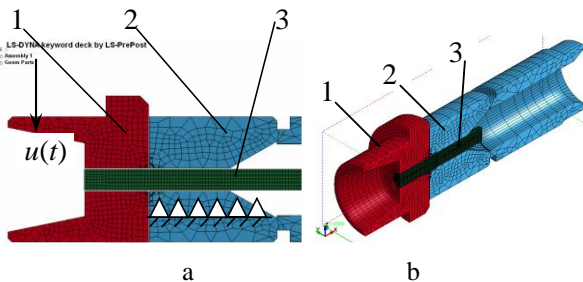


Fig. 4 FEM model with cutting tool description. a - section view, b - isometric view

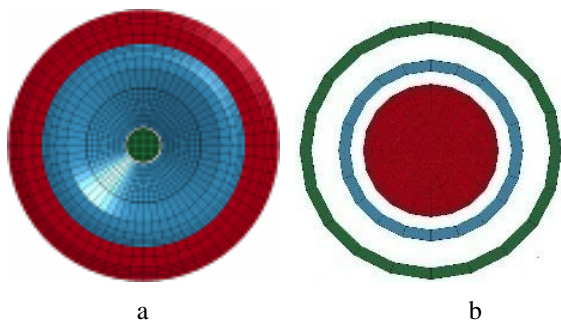


Fig. 5 Proposed cutting tool shapes: a - normal (oval) shape, b - hybrid

matrix configuration: 1 matrix is equal to diameter of cutting material as well as diameter of the punch. The 2-nd matrix is 15% bigger than cutting material. The 3-rd matrix 24% bigger then initial matrix diameter. The 4-th matrix is 32% bigger then initial matrix diameter. And the 5-th matrix is 39% bigger then initial matrix diameter.

Boundary conditions satisfying experimental problem formulated in the Fig. 6 one end of work piece is fixed in the punch and cannot be moved through another

end in free to move in the Z direction (orthogonal cut [1-6]).

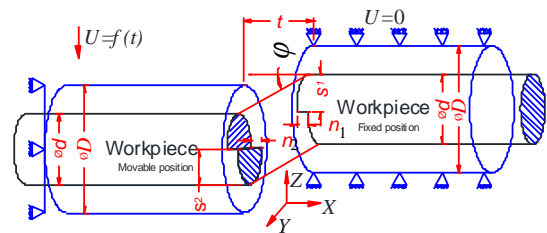


Fig. 6 Boundary conditions

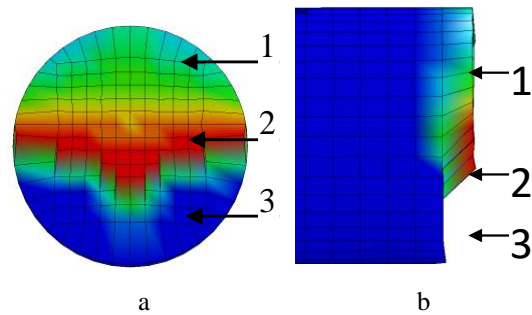


Fig. 7 Wire strip cut with oval shape tools excludes three zones. Numerically cut zone: a - cut zone cross-section view, b - cut zone (side view)

Several unknowns of workpiece are indicated: $\varnothing d$ is diameter of workpiece, $\varnothing D$ is diameter of cutting tools, U is cutting tool displacement as function of time, t is distance between cutting tools, ϕ is rake angle, S_1 and S_2 are an edge of curled edge after cutting operation in orthogonal direction, n_1 and n_2 are curled edge after cutting operation in longitudinal direction. In the present investigation distance between cutting tools was chosen to be without any gap and the influence of this parameter (designated t in the Fig. 6) are not the intensions of this paper and will be presented in the future. FEM of orthogonal cutis given in the Fig. 7. Here in can be seen 3 significant zones. Actual experiment was performed without any gap between tools, though in reality it is impossible to create any cutting tool without a gap. So it will be in a tolerance of around 0.2 mm. All units in calculation and experimental studies are in SI. Though calculation with LS-Dyna are as following: ton, mm, s, N. In the investigation there were used material model from LS-Dyna material library:

*Piece_wise_linear_plasticity, where few modulus where chosen according to equation 1 and 2:

$$E = \frac{d\sigma}{d\varepsilon}, \quad \sigma < \sigma_Y, \quad (1)$$

$$E_{TAN} = \frac{d\sigma}{d\varepsilon}, \quad \sigma > \sigma_Y, \quad (2)$$

where E is Young modulus, $d\sigma$ is true of stress increments, $d\varepsilon$ is true strain increments, σ_Y is yield stress, E_{TAN} is tangent modulus. Final equation of the material model it is used:

$$\sigma_Y (\varepsilon_{eff}^p \dot{\varepsilon}_{eff}^p) = \sigma_Y^s (\varepsilon_{eff}^p) \left[1 + \left(\frac{\dot{\varepsilon}_{eff}^p}{C} \right)^{1/p} \right], \quad (3)$$

here σ_Y is yield stress, ε_{eff}^p is effective plastic strain, $\dot{\varepsilon}_{eff}^p$ is effective plastic strain rate, σ_Y^s is static stress component, C is constant, p is Cowper and Symonds coefficient.

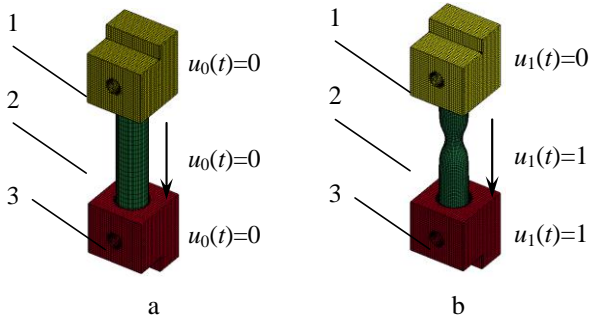


Fig. 8 Tension test apparatus for numerical calculations: a - before tension, b - after tension

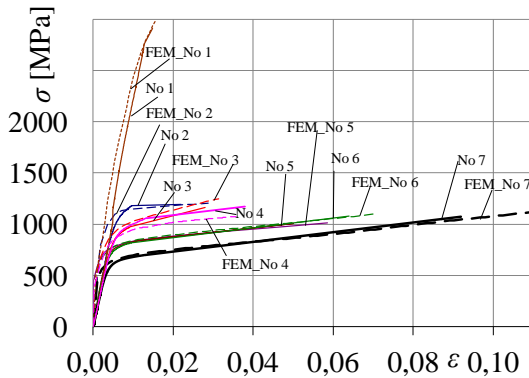


Fig. 9 Tension curves in comparison between different diameters wires. Curves are given in true stress strain coordinates system

Tension test apparatus can be seen in the Fig. 8. To fully matched FEM with experimental investigation there were chosen experimental mechanical curves use in the FEM and do the same tension test but this time numerically [7]. Numerical tension test investigations were made with software LS-Dyna using single precision solver and 64 bit system [4]. Experimental curves from tension test and curves from FEM can be seen in the Fig. 9. The highest mismatched between two methodologies are gained then was testing material No. 4 and this is 8.93%. Other specimens are situated below this value. The average stress component from experiments are 1122 MPa. From finite element analysis stress component are only 5 MPa

(the percentage expression is 2.83).

4. Results

To compare and relate methodologies (experimental and numerical) there were made an investigation of cross-section area (A , A' , A'') measurement. The cross-section where measured in the real specimen after 3D scanned (Fig. 3, a) and also cross-section area (A'') data, taken from FE model. The comparison of cross-section area where made in relation with theoretical data (A). The results are provided in the Fig. 10. Here in one can see specimens' cross-section A measured in mm^2 dependence on the specimens' initial diameter d , mm. Designation $A'-d$ means, that measurements were taken from 3D scanned view. Curve $d-A$ means theoretical cross-section area, without deformation. The 3rd curve $d-A''$ means the same cross-section

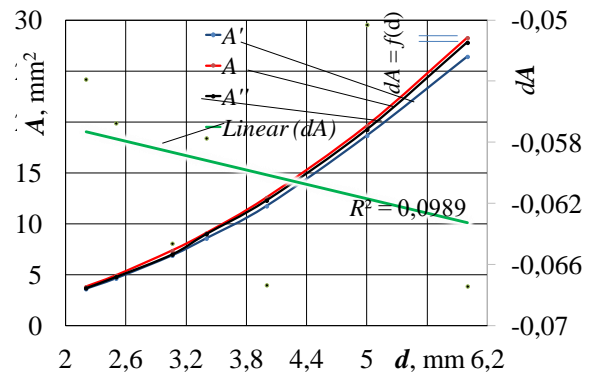


Fig. 10 Experimental measurements of cross section view. A – theoretical area of cross section, A' – measured area, A'' – FEM data, dA – cross-section deformation

area dependence on initial diameter, but data are taken from FE model. The difference of measured data from 3D scan and data taken from FEM is in between 4 percent. So this FEM data we treating as reliable. True strain of a particular cross-section also is given in the Fig. 10. Cross-section deformation (dA) dependence from a value of diameter (d) do not revealed any significant deviation from a nominal value and it can be treated as linear. Though the measurements were made at the final stage of cutting and it might be possible that nonlinearity of cross-sectional area can be obtained in between the cutting operation stages. This can be perfectly be grasped from the Fig. 11 - Fig. 15 where were obtained nonlinearity in between cutting stages. Higher and this fully satisfies an investigation data precision [9, 10]. Experimental cross-sectional view with problematic areas are given in the Figs. 3, b and 4. Numerical analogue view are given in the Fig. 7 the 3 zones are clear. In the experimental view only 2 zones can be identified from the picture.

Though the 3-rd zone can be derived at very endings of the cross-sectional view. After the experimental studies of all diameters wires were completed we examined the most critical place of the wire strip where most likely the fracture will occur [11, 12]. We examined the overall change of area A (listed by the numbers I-V) in parallel with major stress component σ_1 (listed by the numbers 1-5) (Figs. from 11 to 15).

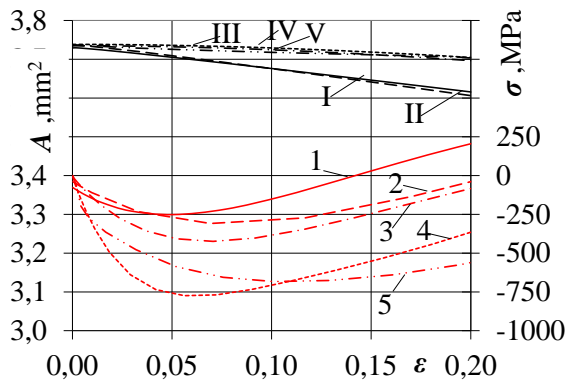


Fig. 11 Reduction of cut area vs. plastic strain in the most deformed element in comparison with major stress at the same element. Wire diameter 2.2 mm

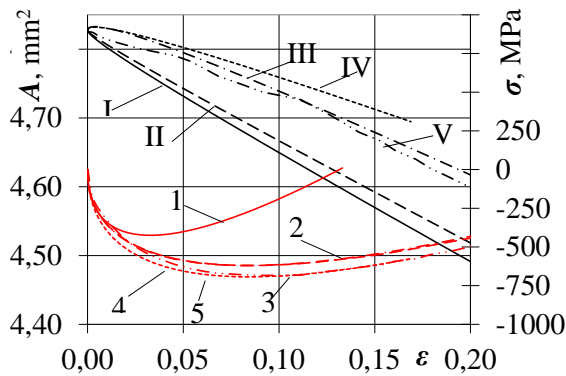


Fig. 12 Reduction of cut area vs. plastic strain in the most deformed element in comparison with major stress at the same element. Wire diameter 2.5 mm

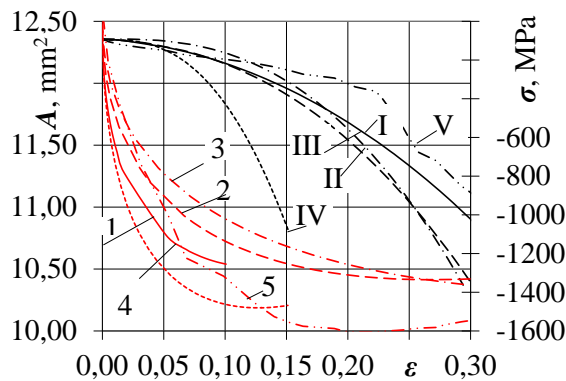


Fig. 13 Reduction of cut area vs. plastic strain in the most deformed element in comparison with major stress at the same element. Wire diameter 4 mm

The common axis of abscises designated for plastic strain $[\epsilon_{pl}]$ distribution. The results from Figures show some common features of wire strip cutting operation. Then diameter of matrix is equal or slightly bigger than the diameter of wire strip (designated 1 and I in the Figs. 11–15) the bending operation begins and plastic deformation are growing straight forward depending on the position of the punch. In the major stress intensity σ_1 shows all investigated diameters influenced wire in the context of bending. The differences between ratio of matrix and the punch shows that increasing matrix diameter proportionally give the wire experiences fracture not at the same stress level, though the plastic deformation $[\epsilon_{pl}]$ component. The

change of are visible only for I and II matrix configuration. And there is no any major distinction between those two. Fig. 9 shows little difference between previous Figure in context of major stress intensity σ_1 . Only 1 matrix configuration differs from other. 2 - 5 matrix configuration show only minor differences.

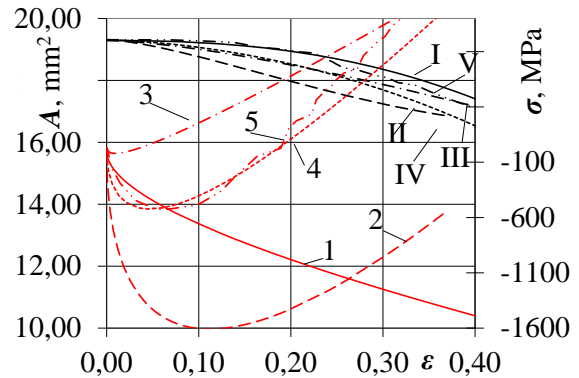


Fig. 14 Reduction of cut area vs. plastic strain in the most deformed element in comparison with major stress at the same element. Wire diameter 5 mm

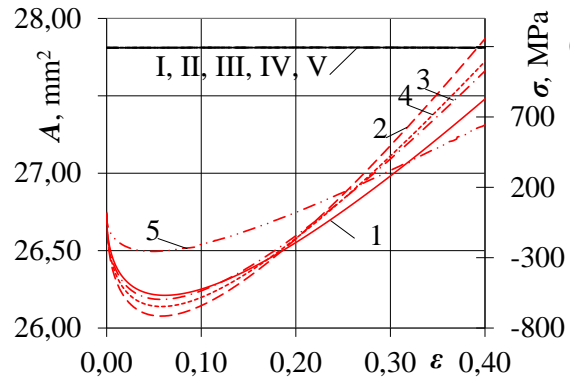


Fig. 15 Reduction of cut area vs. plastic strain in the most deformed element in comparison with major stress at the same element. Wire diameter 6 mm

Though area of the cut cross section have had an area change and it is quite obvious. The reduction of cross sections are: for the matrix I is 14%, II - 13%, III - 7%, IV - 3% and V - 5%. Figure 11 revealed that major stress component has a negative sign, what means that fracture in the cut area begins after compression of wire strip between cutting tools. The reduction of cross sections are: for the matrix I is 12%, II - 18%, III - 7.16%, IV - 12% and V - 18%. In the Fig. 11 can be seen a little different view Here in major stress component has unexpected changes between 1st and 5th. Matrix configuration. Matrix 3, 4 and the 5th have a tendency of negative major component until reach a 0.15 ϵ_{pl} and then experience a positive sign i.e. wire strip experience a tension with no compression at all. But since wire strip of diameter 5 has fractured under around 0.12-0.15 of plastic deformation and around 700 MPa of major stress it looks that at the particular case a fracture of wire strip experienced then major stress component had a negative sign not depending on matrix configuration. The reduction of cross section are: I is 15%, II - 13%, III - 16%, IV - 15% and V - 13%. That means that reduction of cross section uphold quit the same rate of reduction between matrix configurations. In the Fig. 12 there are abso-

lute different situation from the Fig. 11. Fracture begins at the compression. And no real reduction of cross section is noticed.

5. Conclusions

1. Seven different diameters wire strips were tested. Mechanical characteristics by tension test were determined. Seven numerical experiments were examined by changing diameters of punch giving a total of 35 different experiment versions.

1. Based on these findings it is recommended to use results in the design of the new metal sheet cutting tools. As well it is recommended to use these findings in manufacturing of wire strips.

2. Diameter of cutting tool does not influence the wire strip endings; though the ratio of tool/wire does influence the wire strip endings.

3. No single shape solution were determined for a better wire strip end shape since all proposed shapes provided quite huge variation of the idle shape.

4. Oval shape of cutting tool gave an inclination at four sides of wire strip and it cannot be considered as a better shape over others.

5. No better cutting shape was determined, since material for wire strips are in the wide range.

References

1. **Gylienė, V.; Ostaševičius, V.** 2013. The validation of FE modeling of orthogonal turning process using copper-symonds material behavior law, *Engineering Transactions* 61(4): 249-263.
2. **Gylienė, V.; Ostaševičius, V.** 2012. Modeling and simulation of a chip load acting on a single milling tool insert, *Strojnicki vestnik - Journal of Mechanical Engineering* 58(12): 716-723. <http://dx.doi.org/10.5545/sv-jme.2011.356>.
3. **Atkins, T.** 2009. *The science and engineering of cutting*, Linacre House, Jordan Hill, Oxford OX2 8DP, UK, 413p.
4. **Bortkevičius, R.; Dundulis, R.** 2014. Various mechanical properties wire strips influencing single core wire rope construction breaking regularities, *Mechanika 2014: Proceedings of 19th International Conference*, April 24, 2014, Kaunas University of Technology, Lithuania / Kaunas University of Technology, Lithuanian Academy of Science, IFTOMM National Committee of Lithuania, Baltic Association of Mechanical Engineering. - Kaunas: Technologija: 75-79.
5. **Kaya, H.; Uçar, M.; Cengiz, A.; Samur, R.; Özyürek, D.; Çalışkan, A.** 2014. Novel molding technique for ECAP process and effects on hardness of AA7075, *Mechanika* 20(1): 5-10. <http://dx.doi.org/10.5755/j01.mech.20.1.4207>.
6. **Raczy, A.** 2011. An Eulerian finite element model of the metal cutting process, 8th European LS-DYNA Users Conference, Strasbourg, France, S 9: 11-26.
7. **Masillamani, D.P.** 2011. Determination of optimal cutting conditions in orthogonal metal cutting using LS-DYNA with design experiments approach, 8th European LS-DYNA Users Conference, Strasbourg, France, S 9: 27-36.
8. **Bagci, E.** 2011. 3-D numerical analysis of orthogonal cutting process via mesh-free method, *International Journal of the Physical Sciences* 6(6): 1267-1282. <http://dx.doi.org/10.5897/IJPS10.600>.
9. **Zouhar, J.; Piska, M.** 2008. Modelling the orthogonal machining process using cutting tools with different geometry, *MM Science Journal*: 50-51.
10. **Villumén, M.F.** 2008. Simulation of metal cutting using smooth particle Hydrodynamics, Bang & Olufsen, Struer, Denmark, 7th European LS-DYNA Users Conference, Banberg, C-III-17- C-III-36.
11. **Chieragatti, R.** 2008. Modelling high speed machining with the SPH method, ISAE, Toulouse, France, 10th European LS-DYNA Users Conference, 9-20.
12. **Limido, J.** 2006. SPH method applied to high speed cutting modelling, *EURODYMAT International Conference on Mechanical and Physical Behaviour of Materials under Dynamic Loading*, DGM, ENSICA, France, 11p.
13. **Limido, J.; Espinosa, C.; Salaün, M.; Lacombe, J.L.** 2007. SPH method applied to high speed cutting modelling, *International Journal of Mechanical Sciences* 49(7): 898-908. <http://dx.doi.org/10.1016/j.ijmecsci.2006.11.005>.
14. **Ambati, S.; Rega, R.** 2013. Simulation of cutting stresses and temperatures on tool geometry at the onset of turning operation by finite element method, *Paripex - Indian Journal of Research* 2(3): 123-125.
15. LS-Dyna keyword user's manual, volume I, version 917, 2007, 2206p.

R. Dundulis, R. Bortkevičius

INVESTIGATION OF CUTTING TOOL DIAMETER INFLUENCING WIRE CUTTING OPERATION ACCURACY USING SEVERAL MATRIX CONFIGURATIONS

Summary

In this paper there are presented several investigations considering the wire cutting tool diameter which does influence on wire cutting operation accuracy when in the cutting operation it is used various matrix configurations.

The investigation consist of true cutting operations, when is used different poison and the matrix diameters for cutting the same wire diameter. The second part of investigation consists of determining the mechanical properties of tested specimens. The third investigation part is building Finite element model and making tension test as well as making cutting operation as well as in the first part. The last one part of investigation consists of making 3D scan and comparing result of FEM and real scanned specimen. The major investigation achievement is that there were determined three deformed zones in the cut wire strip. This is the same result was gained in the FE model as well. So the model showed relevant and reliable results for making judgments on deformed zones in the real specimen.

Keywords: Wire strip, 3D scan, deformed zones.

Received October 23, 2015

Accepted November 12, 2015